Particle size distributions of fault rocks and fault transpression: are they related?

Andrea Billi, Fabrizio Storti and Francesco Salvini
Dipartimento di Scienze Geologiche, Università 'Roma Tre', L.go S.L. Murialdo 1, 00146 Rome, Italy

ABSTRACT

Laboratory experiments on rock faulting show that processes of particle comminution in fault rocks are influenced by several parameters, including fault strike and normal stress across faults. In nature, normal stress across faults increases with increasing transpressional strike of faults. Accordingly, different structural fabrics and particle size distributions are expected for cataclastic rocks that have developed along faults with different transpressional orientations and comparable displacements within regional-scale strike-slip fault zones. Adjacent bands of cataclastic gouge and breccia were analysed from four small-scale fault zones. All have comparable displacements and very similar protolith (i.e. shallow-water limestone), structure, kinematics, size, and tectonic environment, but different transpressional strikes within the regional-scale left-lateral Mattinata strike-slip fault, Italy. An inverse linear relationship is found between fault transpressional angles and fractal dimensions of particle size distributions from cataclastic rock samples.

Terra Nova, 15, 61–66, 2003

Introduction

Rock fragmentation plays an important role in a variety of natural processes such as tectonic faulting/fracturing, weathering, volcanic explosions and impacts (e.g. Hartmann, 1969; Curran *et al*., 1977; Fujiwara *et al*., 1977; Atkinson, 1987; Hooke & Iverson, 1995). Rock comminution along faults produces lenses and bands of cataclastic rocks, also known as fault cores (Chester *et al*., 1993; Caine *et al*., 1996). The physical properties of fault cores are of considerable social importance because they influence storage and recovery of hydrocarbon and groundwater from faulted strata (e.g. Antonellini and Aydin, 1994, 1995; Caine *et al*., 1996), flows of chemical and radioactive contaminants through rocks (National Research Council, 1996, 2000), and friction along seismic faults (Byerlee, 1978; Allègre *et al*., 1982; Sibson, 1986). For these reasons, several studies have been performed on the parameters controlling the evolution of fault cores (e.g. Jones *et al*., 1998; Holdsworth *et al*., 2001). In laboratory experiments, several authors have demonstrated that cataclasis is a pressure-sensitive process (Rutter *et al*., 1986; Wong *et al*., 1997; Wibberley *et al*., 2000; Mair *et al*., 2002). Amongst other effects, the rate of gouge formation depends linearly on normal stress (Archard, 1953; Yoshioka, 1986). Accordingly, different structural fabrics and particle size distributions are expected for cataclastic rocks developed along transpressional faults with different strikes within a regional-scale brittle shear zone.

The present contribution explores the relationship between particle size distribution of fault rocks and the fault transpressional angle, i.e. the acute angle that locally a transpressional splay fault forms with the master pure strike-slip fault (Fig. 1). It presents the results of statistical analyses on particle size distributions from four small-scale fault cores (i.e. less than 1 m thick) developed in shallow-water carbonate rocks with different transpressional angles within the regional-scale left-lateral Mattinata strike-slip fault, southern Italy (Fig. 2).

Amongst a variety of statistical relationships used to correlate data on the size distribution of fragments, fractal distributions have been proved to successfully describe particle size populations of fault core cataclastic rocks (e.g. Blenkinsop, 1991). Particle size distributions (i.e. particle number vs. size) are defined as fractal within a given range when

$$\log N \approx -D \log r, \qquad (1)$$

where N is the number of particles with size $\approx r$, and D is the fractal dimension of their distribution, i.e. the slope of the logarithmic function (e.g.

Correspondence: Andrea Billi, Dipartimento di Scienze Geologiche, Università 'Roma Tre', L.go S.L. Murialdo 1, 00146 Rome, Italy. Tel.: +39 06 5488 8016; fax: +39 06 5488 8201; e-mail: billi@uniroma3.it

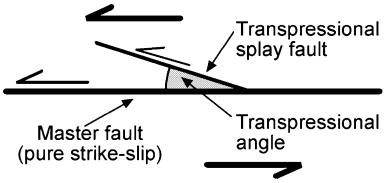

Fig. 1 Schematic diagram (map view) of a strike-slip fault. Note the transpressional angle, i.e the acute angle that locally a transpressional splay fault forms with the master pure strike-slip fault.

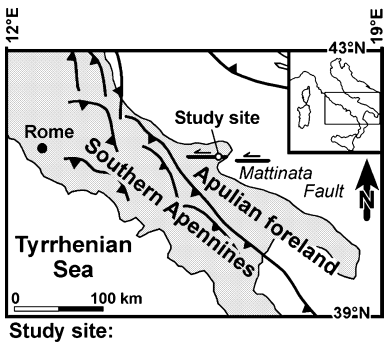

Fig. 2 Location map for the study site: San Simeone Quarries along the Mattinata Fault in the Apulian foreland of the Apennines fold-and-thrust belt, Italy.

Turcotte, 1986). Fractal particle size distributions are scale-invariant, and the fractal dimension provides a means with which to quantify scale invariance (Mandelbrot, 1967). Fractal dimensions of particle size distributions increases with increasing the relative content of finer particles (e.g. Sammis *et al.*, 1986; Turcotte, 1986).

Fault zone structure

The studied fault cores are from four small-scale fault zones (FZ1–4) exposed at the San Simeone Quarries within the damage zone of the Mattinata Fault (Fig. 3a). The Mattinata Fault is an E–W-striking left-lateral strike-slip fault system (Salvini *et al.*, 1999; Billi and Salvini, 2001), which cuts across Mesozoic shallow-water carbonate rocks in the foreland of the Southern Apennines thrust-fold belt (Fig. 2). The Mattinata master fault at the San Simeone Quarries is N92°-striking (Fig. 3a), whereas mesostructural faults strike between N80° and N135° and show strike-slip to slightly oblique-slip slickenlines (Fig. 3b). Solution cleavage occurs as closely spaced subvertical surfaces with a general trend of N120–130° (Fig. 3c). The studied fault zones (Fig. 4) are subvertical (FZ1, FZ3 and FZ4) to high angle (FZ2). Slickenlines on striated fault surfaces indicate strike-slip to slightly oblique-slip movements. The strike of the fault zones varies from N94° to N156° (Fig. 4). By referring to the N92° strike of the Mattinata Fault (Fig. 3b) at the San Simeone Quarries (Servizio Geologico d'Italia, 1970) as the pure strike-slip fault orientation, the transpressional angle of each fault was computed as the acute angle between the strike of the investigated faults and the N92° strike of the Mattinata Fault. These angles fall between 2° and 64° (Table 1). In the case of a transpressional orientation of the Mattinata master fault at the San Simeone Quarries (Salvini *et al.*, 1999), the computed transpressional angles would be increased by the same amount. This will not affect the trend of the relationship hereafter discussed between particle size distributions of fault rocks and the fault transpressional angle.

The analysed fault zones show the same asymmetrical structural architecture (Fig. 4), comprising: (i) the damage zone, which contains solution cleavages and extensional fractures that dissect the cleavage domains at high angle; (ii) the fault surface, which separates the damage zone from the fault core at one side of the fault core; (iii) the fault core, enclosed on both sides by the damage zone and consisting of two adjacent subvertical bands: the gouge zone, adjacent to the fault surface, and the breccia zone, in between the gouge zone and the damage zone.

The thickness of the fault cores ranges between 0.035 m (FZ1) and 0.760 m (FZ4). The thickness of the gouge zones is between 2 and 3% (FZ4) and 85% (FZ2) of the thickness of the respective fault cores (Table 1). The actual displacement of the analysed faults could not be measured. However, by referring to the relationship between fault displacement and gouge zone thickness (fig. 2 in Scholz, 1987; reference therein), a comparable displacement on the order of 1 m could be estimated for all the analysed faults.

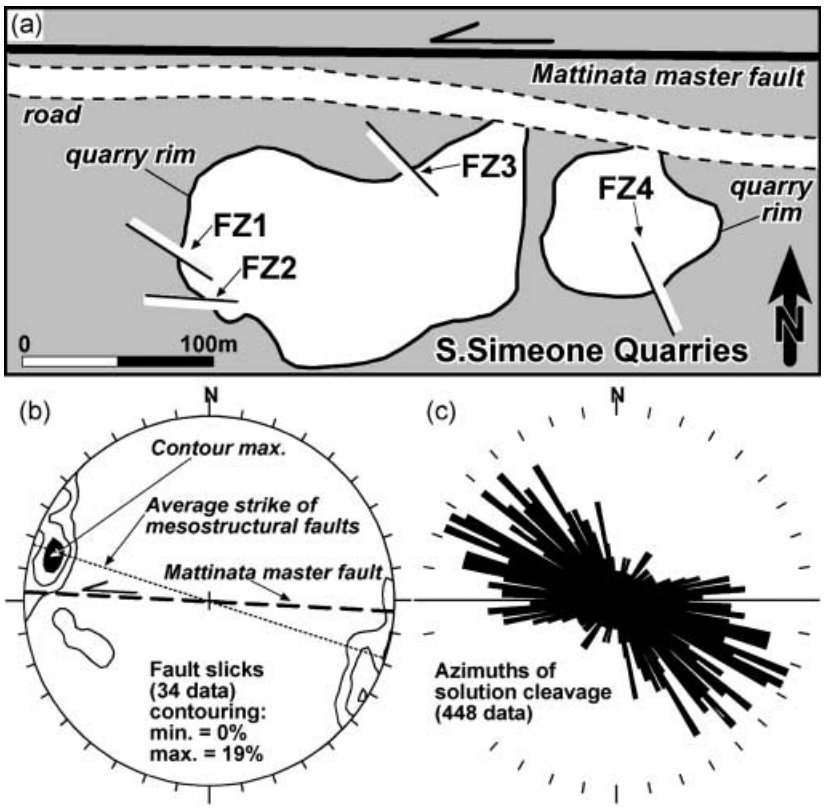

Fig. 3 (a) Location map for the fault zones studied within the San Simeone Quarries. (b) Contouring to fault slicks (Schmidt net, lower hemisphere) collected in the San Simeone Quarries area. (c) Histogram (rose diagram) of solution cleavage azimuths collected in the San Simeone Quarries area.

Methods

Particle size distributions of carbonate cataclastic rocks from fault cores were determined by using a sieving-and-weighting technique (e.g. Exner, 1972; Sammis *et al.*, 1986; Hooke and Iverson, 1995) adapted as follows (Storti *et al.*, 2001). (i) Samples were disaggregated in a nondestructive ultrasonic device and sieved by using a standard seven sieve array with mesh apertures of 4.000×10^{-3}, 2.000×10^{-3}, 1.000×10^{-3}, 0.500×10^{-3}, 0.250×10^{-3}, 0.125×10^{-3} and 0.063×10^{-3} m. (2) By assuming a nearly spherical geometry of rock clasts (e.g. Hooke and Iverson, 1995), the number of equivalent spherical particles was determined by dividing the weight of the residue in each sieve (i.e. except the residue in the largest sieve that contains all larger particles) into the weight of the reference spheres

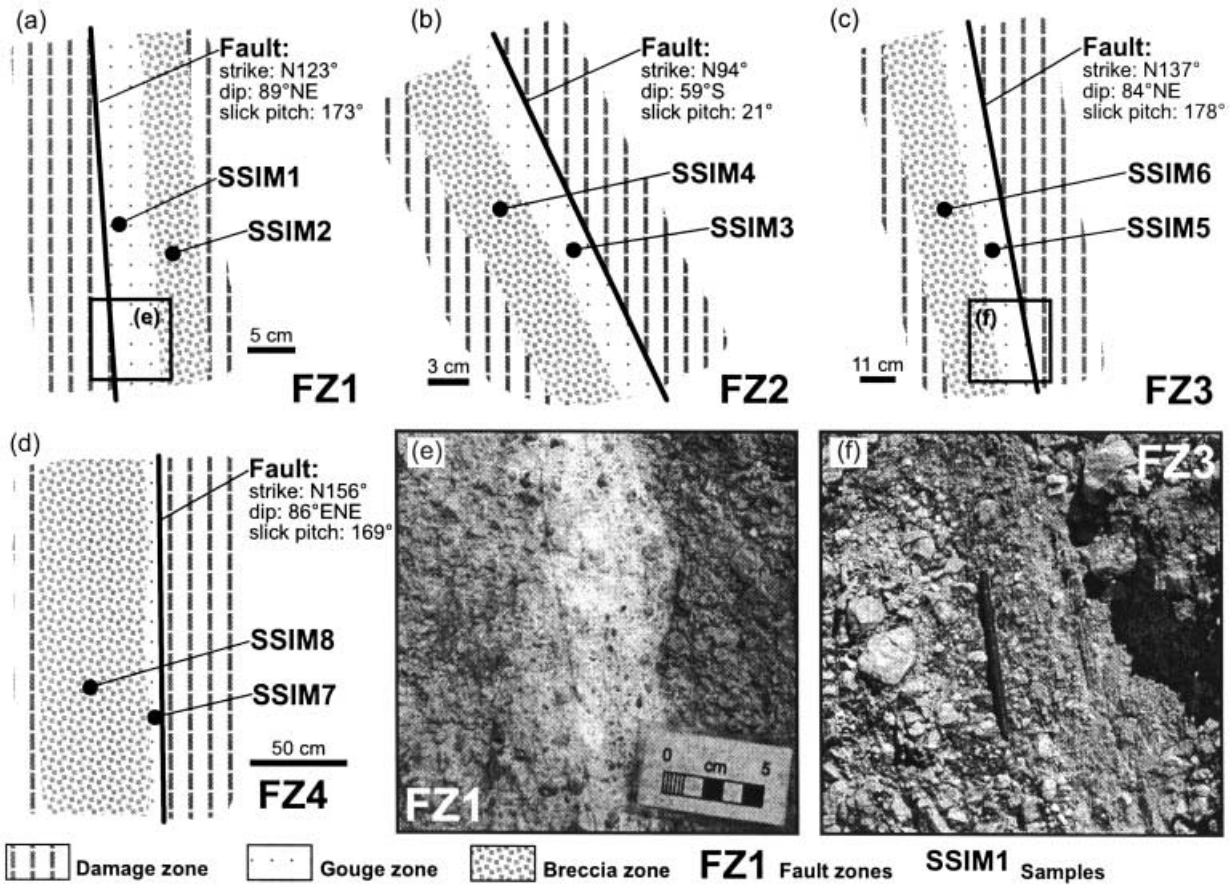

Fig. 4 Schematic sections of the fault zones studied: (a) FZ1, (b) FZ2, (c) FZ3 and (d) FZ4. Photographs from the fault zones: (e) FZ1 and (f) FZ3.

Table 1 Summary of fault zone structural parameters

	Fault zones			
	FZ1	**FZ2**	**FZ3**	**FZ4**
Fault strike	N123°	N94°	N137°	N156°
Fault dip	89°NNE	59°S	84°NE	86°ESE
Slick pitch	173°	21°	178°	169°
Kinematics	strike-slip	strike-slip	strike-slip	strike-slip
Transpressional angle	31°	2°	45°	64°
Fault core thickness	0.100 m	0.035 m	0.140 m	0.760 m
Gouge thickness	0.050 m	0.030 m	0.045 m	0.020 m

having the density of a pure limestone (Turcotte and Schubert, 1982) and the diameter equal to the mesh aperture of the next larger sieve. From this processing the number of equivalent spherical particles corresponding to the following six classes of size was obtained: 4.000×10^{-3}, 2.000×10^{-3}, 1.000×10^{-3}, 0.500×10^{-3}, 0.250×10^{-3} and 0.125×10^{-3} m. (iii) The number of equivalent spherical particles was projected against the corresponding size rank in log–log graphs, and data were fitted with a power-law best fit of the type

$$\log(y) = -D\log(x) + A, \quad (2)$$

where D is the fractal dimension of the analysed particle size range.

Particle size distribution

The fault cores studied (Fig. 4) consist of uncemented to poorly cemented cataclastic rocks with grain sizes generally less than 0.001 m in the gouge zone, and less than 0.004 m in the breccia zone. The gouges are very weak and friable with no foliations, whereas the tight packing of coarse breccia clasts give the breccia zones stronger frictional properties. On approaching the gouge zones, breccia clasts show evidence of slight translation/rotation with respect to one another and clast packing becomes looser. In each fault zone, one sample was taken from the gouge zone and one from the adjoining breccia zone (Fig. 4). Sample weights vary between 285.77 and 1787.26 g. Data from the analysed samples are listed in Table 2. In Fig. 5, the number of equivalent spherical particles of each sample is plotted against the corresponding size rank on log–log graphs. On these graphs, the log–log distributions of data are satisfactorily fitted by a linear function (i.e. the correlation

Table 2 List of data used for analyses of particle size distribution. Note that D is the fractal dimension

Fault zone	Sample	D	Weight (g)	No. of equivalent spherical particles by diameter					
				4 mm	2 mm	1 mm	0.5 mm	0.25 mm	0.125 mm
FZ1	SSIM1	2.678	285.77	50	317	2051	13 755	98 597	482 057
FZ1	SSIM2	2.392	796.41	218	936	3972	19 564	111 816	986 546
FZ2	SSIM3	3.040	626.65	69	732	6474	55 372	392 215	2638 267
FZ2	SSIM4	2.791	1276.44	216	1881	13 491	93 719	608 523	3481 066
FZ3	SSIM5	2.463	741.82	187	1118	6024	34 464	183 862	961 368
FZ3	SSIM6	2.128	1787.26	304	1592	6160	21 775	87 197	367 611
FZ4	SSIM7	2.233	979.36	358	2129	10 424	48 262	206 694	861 568
FZ4	SSIM8	2.009	972.20	685	3573	15 995	66 259	276 965	1155 472

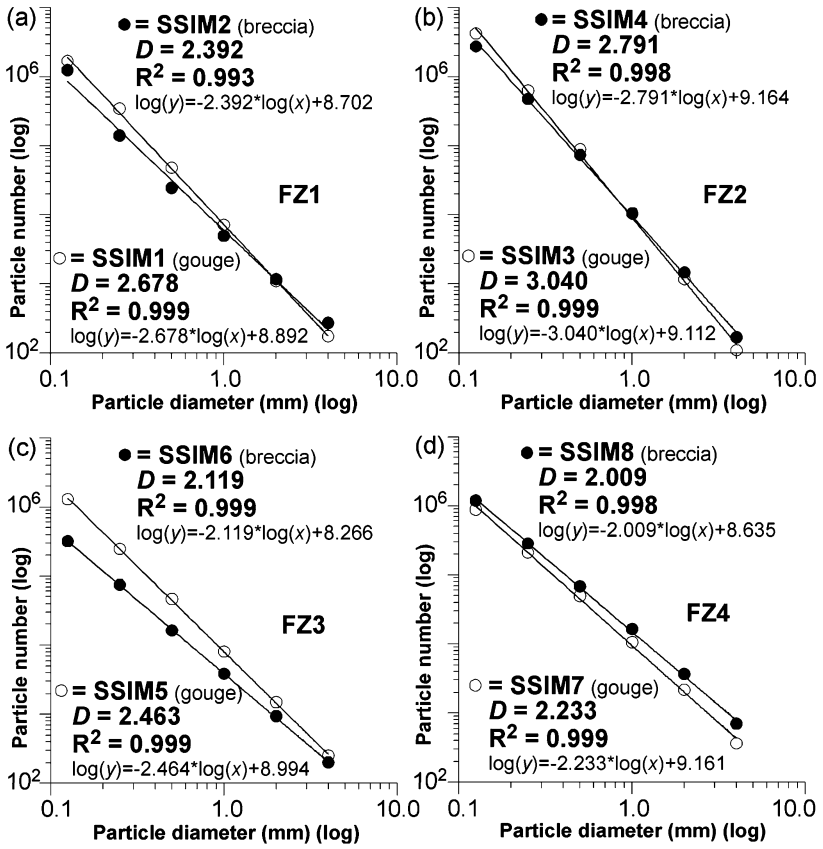

Fig. 5 Log–log graphs of the number of equivalent spherical particles (ordinate) against the particle diameter (abscissa), for the fault zones studied: (a) FZ1, (b) FZ2, (c) FZ3 and (d) FZ4. Note that D is the fractal dimension and R^2 is the correlation coefficient.

coefficient, R^2, is between a minimum of 0.993 and a maximum of 0.999). The fractal dimension, D, is between a minimum of 2.009 (SSIM6) and a maximum of 3.040 (SSIM3). Samples from the gouge zones, being finer-grained, have D-values always greater than samples from the corresponding breccia zone (Fig. 5).

Note that owing to the limited range of size investigated (from 4.000×10^{-3} to 0.125×10^{-3} m), the fractal dimensions from the studied particle size distributions can exceed the theoretical limit of 3, i.e. a distribution with $D = 3$ over the entire size range of the sample would completely fill the available volume (Steacy and Sammis, 1992).

Fault transpressional angle vs. D-value

Figure 6(a) shows the relationship between the fault transpressional angles and the corresponding D-values. The relationship is linear for both the gouge and the breccia series. D-values increase as the transpressional angle decreases from 64° (FZ4) to 2° (FZ2). The direction coefficients computed from the two linear fits are very similar, i.e. 73.852 for the breccia series and 76.048 for the gouge series. Accordingly, a roughly linear relationship exists also between D-values from the gouge series and D-values from the corresponding breccia series (Fig. 6b).

Discussion

Fractal dimensions from the studied particle size distributions of fault rocks show an inverse linear correlation with the fault transpressional angles. This relationship applies to both the gouge and the breccia series.

In the breccia series, where bulk crushing of particles prevails over particle grinding (e.g. Hattori and Yamamoto, 1999), a physical explanation for the occurrence of this relationship can be found in the progressive increase of the normal stress across faults with increasing transpressional angle (e.g. Sanderson and Marchini, 1984). Such a stress increase, in fact, raises the rock resistance to macroscopic failure (Jaeger and Cook, 1979; Turcotte, 1986) and, consequently, influences the fracture density in the rock volume from which the prospective fault core nucleates. Fracture density, in turn, controls the shape and size of particles in the early stages of fault core evolution, i.e. before rotation-enhanced particle grinding.

Unlike breccia, gouge develops mainly by particle grinding during fault slip – it is a displacement-sensitive process (Marone and Scholz, 1989) – probably by reworking an earlier breccia (e.g. Hattori and Yamamoto, 1999). The parallel relationships between the fault transpressional angle and the fractal dimensions from the gouge and the breccia particle size distributions indicate that the mechanism of particle grinding that led to the formation of

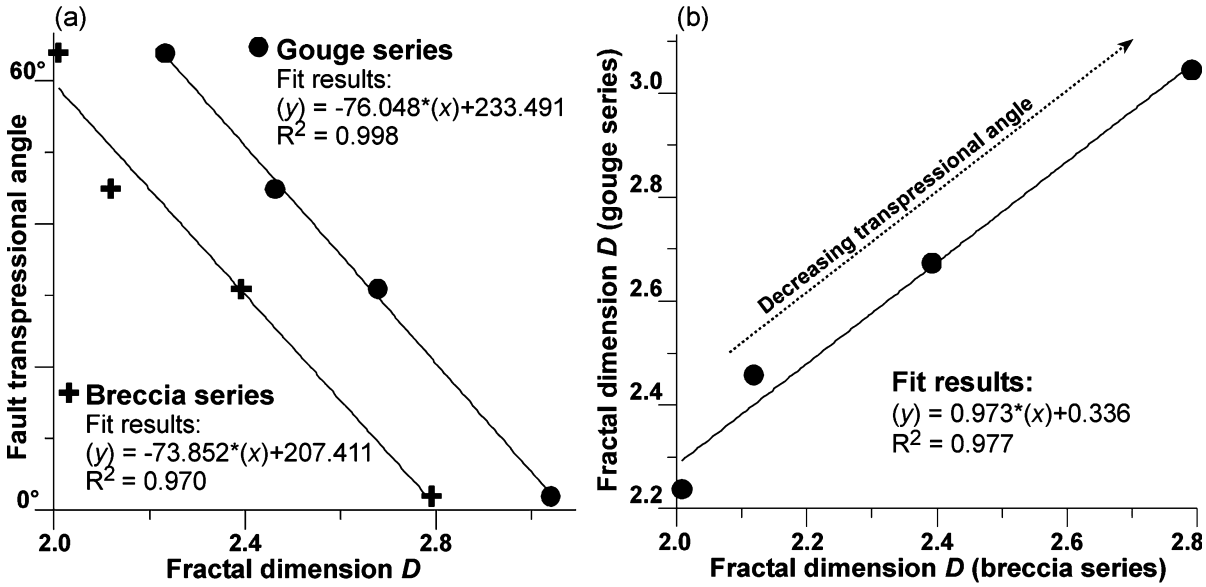

Fig. 6 Graphs depicting the relationship between (a) transpressional angles and *D*-values from both the gouge and the breccia series, and (b) *D*-values from the gouge series (ordinate) and *D*-values from the corresponding (i.e. same fault zone) gouge series (abscissa). Note that *D* is the fractal dimension and R^2 is the correlation coefficient.

the gouge zones is sensitive to the initial rock fabric (i.e. the fractal dimension of the breccia). However, it is less sensitive to the fault transpressional angle – regardless of the transpressional angle, in fact, the difference between *D*-values from the gouge and the breccia series is between 0.2 and 0.3 in all the fault cores. This provides further support to the inference that the displacements on the faults studied are comparable.

Amongst other factors, fault displacement strongly influences the particle size distributions of fault rocks (e.g. Engelder, 1974; Yoshioka, 1986; Blenkinsop, 1991). The resolution of the displacement-to-gouge thickness relationship used to assess the displacement on the studied faults (Scholz, 1987), is insufficient to appraise very low amounts of displacement. This means that the displacements estimated from the respective gouge thickness, despite being comparable on the order of 1 m, may differ by up to centimetres. Laboratory experiments (e.g. Mandl *et al*., 1977; Marone and Scholz, 1989) suggest that even such a low amount of displacement discrepancy may have played a role in the final particle size distribution, regardless of transpressional angle. For this reason, further validation is needed on faults in which displacement can be better constrained.

Conclusions

1 Particle size distributions from eight samples of carbonate fault rocks collected within four small-scale fault cores are well fitted by power-law functions over the 4.000×10^{-3} to 0.125×10^{-3} m size range.

2 The fractal dimension (*D*) of particle size distributions is between a minimum of 2.009 and a maximum of 3.040. In each fault core, the value of *D* from the gouge sample is greater than the value of *D* from the breccia sample. In all the studied fault cores their ratio is about 0.97, and their difference is about 0.2–0.3, regardless of the fault transpressional angle.

3 *D*-values are greater for samples from fault cores with lower transpressional angles. This relationship is linear for both the gouge and the breccia series, and parallel between them.

4 The fractal dimension-to-transpressional angle relationship, although preliminary, has implications for the assessment of permeability and friction across transpressional faults. In particular, this study shows that the production of gouge along faults and its particle size properties are sensitive to the inherited rock fabrics, which, in turn, are influenced by the fault transpressional angle.

Acknowledgments

We are in debt to the Geo-tectonics mail list whose members provided references on cataclasis and fractal analysis of fragmentation processes. Suggestions from D. Peacock, C. Wibberley and the editor, A. Nicolas, significantly improved this paper.

References

Allègre, C.J., Le Mouel, J.L. and Provost, A., 1982. Scaling rules in rock fracture and possible implications for earthquake predictions. *Nature*, **297**, 47–49.

Antonellini, M. and Aydin, A., 1994. Effect of faulting on fluid flow in porous sandstones: petrophysical properties. *Bull. Am. Ass. Petrol. Geol.*, **78**, 355–377.

Antonellini, M. and Aydin, A., 1995. Effect of faulting on fluid flow in porous sandstones: geometry and spatial distribution. *Bull. Am. Ass. Petrol. Geol.*, **79**, 642–671.

Archard, J.F., 1953. Contact and rubbing of flat surfaces. *J. Appl. Phys.*, **24**, 981–988.

Atkinson, B.K. (ed.), 1987. *Fracture Mechanics of Rock*. Academic Press, London.

Billi, A. and Salvini, F., 2001. Fault-related solution cleavage in exposed carbonate reservoir rocks in the southern Apennines, Italy. *J. Petrol. Geol.*, **24**, 147–169.

Blenkinsop, T.G., 1991. Cataclasis and processes of particle size reduction. *Pure Appl. Geophys.*, **136**, 59–86.

Byerlee, J.D., 1978. Friction of rocks. *Pure Appl. Geophys.*, **116**, 615–626.

Caine, J.S., Evans, J.P. and Forster, C.B., 1996. Fault zone architecture and permeability structure. *Geology*, **24**, 1025–1028.

Chester, F.M., Evans, J.P. and Biegel, R.L., 1993. Internal structure and weakening mechanisms of the San Andreas Fault. *J. Geophys. Res.*, **98**, 771–786.

Curran, D.R., Shockey, D.A., Seaman, L. and Austin, M., 1977. Mechanisms and models of cratering in earth media. In: *Impact and Explosion Cratering* (D.J. Roddy *et al.*, eds), pp. 1057–1087. Pergamon Press, New York.

Engelder, J.T., 1974. Cataclasis and the generation of fault gouge. *Bull. Geol. Soc. Am.*, **85**, 1515–1522.

Exner, H.E., 1972. Analysis of grain- and particle-size distributions in metallic materials. *Int. Metallurg. Rev.*, **17**, 25–42.

Fujiwara, A., Kamimoto, G. and Tsukamoto, A., 1977. Destruction of basaltic bodies by high-velocity impact. *Icarus*, **31**, 277–288.

Hartmann, W.K., 1969. Terrestrial, lunar and interplanetary rock fragmentation. *Icarus*, **10**, 201–213.

Hattori, I. and Yamamoto, H., 1999. Rock fragmentation and particle size in crushed zones by faulting. *J. Geol.*, **107**, 209–222.

Holdsworth, R.E., Strachan, R.A., Magloughlin, J.F. and Knipe, R.J. (eds), 2001. The nature and tectonic significance of fault zone weakening. *Spec. Publ. Geol. Soc. London*, **186**, 1–342.

Hooke, R., Le, B. and Iverson, N.R., 1995. Grain-size distribution in deforming subglacial tills: role of grain fracture. *Geology*, **23**, 57–60.

Jaeger, J.C. and Cook, R.G.W., 1979. *Fundamentals of Rock Mechanics*. Halstead Press, New York.

Jones, G., Fisher, Q.J. and Knipe, R.J., (eds), 1998. Faulting, fault sealing and fluid flow in hydrocarbon reservoirs. *Spec. Publ. Geol. Soc. London*, **147**, 1–319.

Mair, K., Elphick, S. and Main, I., 2002. Influence on confining pressure on the mechanical and structural evolution of laboratory deformation bands. *Geophys. Res. Lett.*, **29**(10), 49–41–49-4.

Mandelbrot, B.B., 1967. How long is the coast of Britain? *Science*, **156**, 636–638.

Mandl, G., de Jong, L.N.J. and Maltha, A., 1977. Shear zones in granular material: an experimental study of their structure and mechanical genesis. *Rock Mechanics*, **9**, 95–144.

Marone, C. and Scholz, C.H., 1989. Particle-size distribution and microstructures within simulated fault gouge. *J. Struct. Geol.*, **11**, 799–814.

National Research Council, 1996. *Rock Fractures and Fluid Flow: Contemporary Understanding and Applications*. National Academy Press, Washington.

National Research Council, 2000. *Groundwater & Soil Cleanup: Improving Management of Persistent Contaminants*. National Academy Press, Washington.

Rutter, E.H., Maddock, R.H., Hall, S.H. and White, S.H., 1986. Comparative microstructures of natural and experimentally produced clay-bearing fault gouges. *Pure Appl. Geophysics*, **124**, 3–29.

Salvini, F., Billi, A. and Wise, D.U., 1999. Strike-slip fault-propagation cleavage in carbonate rocks: the Mattinata Fault zone. *J. Struct. Geol.*, **21**, 1731–1749.

Sammis, C.G., Osborne, R.H., Anderson, J.L., Banerdt, M. and White, P., 1986. Self-similar cataclasis in the formation of fault gouge. *Pure Appl. Geophys.*, **124**, 53–78.

Sanderson, D.J. and Marchini, W.R.D., 1984. Transpression. *J. Struct. Geol.*, **6**, 449–458.

Scholz, C.H., 1987. Wear and gouge formation in brittle faulting. *Geology*, **15**, 493–495.

Servizio Geologico d'Italia, 1970. *Carta Geologica d'Italia: Map 159, sheet 156: S. Marco in Lamis*, scale 1:100 000. Servizio Geologico d'Italia, Rome.

Sibson, R.H., 1986. Earthquakes and rock deformation in crustal fault zones. *Ann. Rev. Earth Planet. Sci.*, **14**, 149–175.

Steacy, S.J. and Sammis, C.G., 1992. A damage mechanics model for fault zone friction. *J. Geophys Res.*, **97**, 587–594.

Storti, F., Billi, A. and Salvini, F., 2001. Particle size analysis in carbonate fault rocks: inferences for non self similar cataclasis during fault core evolution. In: *European Geophysical Society, XXVI General Assembly, 25–30 March 2001, Nice*, p. 59. European Geophysical Society, Nice.

Turcotte, D.L., 1986. Fractals and fragmentation. *J. Geophys. Res.*, **91**, 1921–1926.

Turcotte, D.L. and Schubert, G., 1982. *Geodynamics: Applications of Continuum Physics to Geological Problems*. Wiley, New York.

Wibberley, C.A.J., Petit, J.-P. and Rives, T., 2000. Micromechanics of shear rupture and the control of normal stress. *J. Struct. Geol.*, **22**, 411–427.

Wong, T.-F., David, C. and Zhu, W., 1997. The transition from brittle faulting to cataclastic flow in porous sandstones: mechanical deformation. *J. Geophys. Res.*, **102**, 3009–3025.

Yoshioka, N., 1986. Fracture energy and the variation of gouge and surface roughness during the frictional sliding of rocks. *J. Phys. Earth*, **34**, 335–355.

Received 25 July 2002; revised version accepted 22 October 2002

